BMC Psychiatry

RESEARCH

Open Access

# The role of senescence-related genes in major depressive disorder: insights from machine learning and single cell analysis

Kun Lian[1,2†], Wei Yang[2,3,4†], Jing Ye[2], Yilan Chen[3,4], Lei Zhang[3,4] and Xiufeng Xu[2,5*]

## Abstract

**Background** Evidence indicates that patients with Major Depressive Disorder (MDD) exhibit a senescence phenotype or an increased susceptibility to premature senescence. However, the relationship between senescence-related genes (SRGs) and MDD remains underexplored.

**Methods** We analyzed 144 MDD samples and 72 healthy controls from the GEO database to compare SRGs expression. Using Random Forest (RF) and Support Vector Machine-Recursive Feature Elimination (SVM-RFE), we identified five hub SRGs to construct a logistic regression model. Consensus cluster analysis, based on SRGs expression patterns, identified subclusters of MDD patients. Weighted Gene Co-expression Network Analysis (WGCNA) identified gene modules strongly linked to each cluster. Single-cell RNA sequencing was used to analyze MDD SRGs functions.

**Results** The five hub SRGs: *ALOX15B*, *TNFSF13*, *MARCH 15*, *UBTD1*, and *MAPK14* showed differential expression between MDD patients and controls. Diagnostics models based on these hub genes demonstrated high accuracy. The hub SRGs correlated positively with neutrophils and negatively with T lymphocytes. SRGs expression pattern revealed two distinct MDD subclusters. WGCNA identified significant gene modules within these subclusters. Additionally, individual endothelial cells with high senescence scores were found to interact with astrocytes via the Notch signaling pathway, suggesting a specific role in MDD pathogenesis.

**Conclusion** This comprehensive study elucidates the significant role of SRGs in MDD, highlighting the importance of the Notch signaling pathway in mediating senescence effects.

**Keywords** Bulk RNA analysis, Major depressive disorder, Senescence, Single-cell RNA analysis, Endothelial cells

†Kun Lian and Wei Yang first authors.

*Correspondence:
Xiufeng Xu
xfxu2004@sina.com
[1] Department of Neurosurgery, The Second Affiliated Hospital of Kunming Medical University, Kunming, Yunnan 650101, China
[2] Department of Psychiatry, The First Affiliated Hospital of Kunming Medical University, No.295, Xichang Road, Wuhua District, Kunming, Yunnan 650000, China
[3] Department of Psychiatry, The Second People's Hospital of Yuxi, No. 4, Xingyun Road, High-tech Development Zone, Yuxi, Yunnan 653100, China
[4] Yuxi Hospital, Kunming University of Science and Technology, Yuxi, Yunnan 653100, China
[5] Yunnan Clinical Research Center for Mental Disorders, Kunming, Yunnan 650000, China

## Introduction

Major Depressive Disorder (MDD) affects over 300 million people worldwide, with an annual prevalence rate of 4.4% [1]. It is the leading cause of disability globally and ranks as the third highest in terms of illness burden [2]. MDD is characterized by persistent depression, diminished of interest in activities, and cognitive slowing. Severe cases can lead to suicide or self-harm. Despite its prevalence, the exact pathophysiological mechanisms underlying MDD remain unclear. MDD results from a complex interplay of gut microbiota, immune function, neuroendocrine systems, genetics, psychosocial factors, and other variables [3, 4]. Understanding the fundamental processes, identifying reliable biomarkers, improving diagnostic accuracy, and reducing the overall healthcare burden are crucial for benefiting both patients and society [5].

Biological senescence typically halts the cell cycle in the G0 and G1 phases, thereby permanently inhibiting cell proliferation. Senescent cells exhibit distinct morphological features, including cell flattening, nuclear enlargement, and chromatin aggregation [6]. Thsee cells also possess a secretory phenotype, releasing various cytokines, chemokines, growth factors, and matrix metalloproteinases [7]. Beyond psychopathological aspects, MDD is linked to biological senescence, evidenced by shortened telomeres and age-related brain changes [8–10]. MDD is associated with cardiovascular, cerebrovascular, and metabolic issues [11], and it increases the risk of Alzheimer's disease, other dementias, frailty, and a reduced lifespan [12–14].

Clinical and epidemiological data suggest a connection between MDD and aging, although the underlying mechanisms are not fully understood. This study employs bioinformatics to investigate the association between MDD and SRGs. We analyzed transcriptomic data from MDD patients and healthy controls to identify differentially expressed genes associated with senescence. Using support vector machines (SVMs) and random forests (RF), we identified 5 hub SRGs to develop a diagnostic model. We evaluated the model's diagnostic performance and examined the relationship between these diagnostic genes and immune cell infiltration. SRGs were used to identify molecular subtypes of MDD. WGCNA analysis revealed tightly connected gene modules within these subclusters. At the single-cell level, endothelial cells with high senescence scores were found to interact with astrocytes via the Notch signaling pathway, indicating diverse roles in MDD progression. This study enhances our understanding of the role of senescence in MDD and lays the groundwork for future research and therapeutic advancements.

## Materials and methods

### Data collection and pretreatment

We obtained MDD gene expression profile datasets, GSE32280 and GSE98793, from the GEO database. GSE98793 included 128 MDD patients and 64 healthy controls, while GSE32280 comprised 16 MDD patients and 8 healthy controls. Both datasets were generated using the GPL570 platform (Affymetrix Human Genome U133 Plus 2.0 Array) [15, 16]. After normalizing the datasets, we combined them using the R package "sva" resulting in a final sample of 144 MDD patients and 72 healthy controls [17]. We sourced 279 SRGs from the Human Aging Genomic Resources, (https://genomics.senescence.info/) [18], as detailed in Supplementary Table 1.

### Differential expression analysis

The "limma" R software package was utilized to identify genes that were significantly differentially expressed between depressed patients and healthy controls and potentially contributing to the pathogenesis of MDD [19]. DEGs were selected based on a $p$-value < 0.05 and an absolute Log2FC > 1.5. Heatmaps and volcano plots were generated using the "heatmap" and "ggplot2" R packages, respectively. We identified SR-DEGs by finding common genes between DEGs and SRGs. Gene Set Variation Analysis (GSVA) is an unsupervised gene set enrichment analysis method that evaluates the variability of gene sets in different samples by calculating the enrichment scores of predefined gene sets in the sample [20].

### Identification of hub genes

Hub SR-DEGs were screened by RF and SVM-RFE analysis [21, 22]. These methods assess the contribution of each gene to disease classification and identify the most discriminative features. We chose these methods for their power and robustness in feature selection. We ranked each SRGs by importance using these methods and selected the top 10 genes from each. The common genes identified by both methods were designated as hub SR-DEGs.

### Construction and validation of the diagnostic model

To evaluate the diagnostic value of the hub genes for depression, the "pROC" package was employed to generate the receiver operating characteristic (ROC) curve and compute the area under the curve (AUC) to thereby constructing a diagnostic model [23]. Addiyionally, multivariate logistic regression analysis was performrd on the hub genes. Model stability was assessed using calibration and decision curve analyses, and a nomogram was developed to predict the probability of MDD. Internal validation was performed using the bootstrap method with

1000 replicates, and discrimination was evaluated by the AUC of the ROC curve.

#### Immune cell infiltrate analysis

Immune dysregulation plays a crucial role in the pathogenesis of MDD. To elucidate the characteristics of immune responses in MDD, we analyzed the immune cells infiltration using IOBR and MCPcounter techniques [24, 25]. In addition, Pearson correlation coefficient was used for correlation analysis to explore the relationship between central SRGs and inflammatory factors.

#### Consensus clustering analysis and co-expression analysis

We conducted a consensus cluster analysis to identify distinct subgroups of MDD patients based on SRGs expression and immunological profiles. Consensus cluster analysis was performed using "ConsensusClusterPlus" on MDD samples, evaluating up to 10 clusters [26]. After multiple testing and adjustment, we determined that the optimal number of clusters (k) was 2 (Supplementary Fig. 1). We then analyzed the top 5000 genes with the highest variability and used unsupervised consensus clustering to determine the optimal number of groups. Additionally, WGCNA was used to identify gene modules with highly synergistic changes, a method demonstrated to effectively reveal molecular mechanisms in complex diseases [27]. WGCNA identified gene clusters with similar mRNA expression patterns in MDD samples. The scale-free topology (SFT) criterion established the power adjacency function with a soft threshold parameter, aiming for a model-fit saturation greater than 0.85.

#### Gene set enrichment analysis

Gene set enrichment analysis can explore the biological processes and signaling pathways involved in differentially expressed genes to reveal the potential molecular mechanisms of MDD. We obtained Homo sapiens gene sets from the Molecular Signature Database (MSigDB) using the "msigdbr" R package [28]. Metascape is a Web-based portal that provides comprehensive gene list annotation and analysis resources [29]. Gene set variation analysis (GSEA) was performed using the "GSEA" package with the single-sample gene set enrichment analysis (ssGSEA) approach using a Gaussian kernel cumulative distribution function [30].

#### Basic analysis workflow of scRNA-seq data

To further elucidate the cellular and molecular basis of MDD, comprehensive single-cell assays were employed. High-quality scRNA-seq data were ensured by excluding cells expressing fewer than 300 genes or having less than 20% mitochondrial gene counts. The Cell-Cycle Scoring tool in Seurat (version 4.3.0) categorized cells into different stages cell cycle stages. Data were standardized using the SCTransform function [31]. The Harmony package (version 0.1.1) corrected for batch effects, using the top 2000 variable genes. Elbow and Jackstraw plots guided the selection of principal components. Clusters were identified using shared nearest neighbor (SNN) modularity optimization at a resolution of 0.8, visualized with UMAP, and classified based on gene expression profiles. SRG scores were calculated using UCell V.2.2.0 [32]. These steps are critical for understanding the heterogeneity and cell-specific changes in MDD at the single-cell level.

#### Construction and analysis of the transcription factor-gene network

The SCENIC framework was employed to identify transcription factor regulons from a count matrix of 10,000 variably expressed genes. Genes active in fewer than 1% of cells were excluded [33]. The gene co-expression network was constructed using Arboreto's gradient boosting machine method. Enriched patterns were predicted using pre-computed databases from cisTargetDB and the SCENIC ctx function, with regulon activity scores calculated per cell using AUCell [34].

#### Cell-cell communication analysis

The CellCall software was employed to analyze ligand-receptor-transcription factor (L-R-TF) axes from the KEGG pathway, thereby deducing networks of intracellular communication [35]. This analysis elucidated the mechanisms connecting high- and low-senescence groups to other cell types.

#### Statistical analysis

Raw data processing and statistical analyses were conducted using R version 4.2.1. Significant differences between groups were determined using the Student's t-test, Wilcoxon rank sum test, and Kruskal-Wallis test for unrelated groups. A $p$-value < 0.05 was considered statistically significant.

## Results

#### Differential expression analysis of SRGs between MDD and controls

After eliminating batch effects from the datasets, which included 72 normal controls and 144 MDD samples, we generated a combined gene expression profile comprising 21,755 genes. We identified 2,059 DEGs with a $p$-value < 0.05 and a fold-change greater than 1.5. We identified 33 SR-DEGs by finding common genes between these 2059 DEGs and 279 SRGs. GSVA analysis revealed a significant increase in senescence scores in individuals with MDD compared to controls (Fig. 1A). Among these, 33 SRGs exhibited notable expression

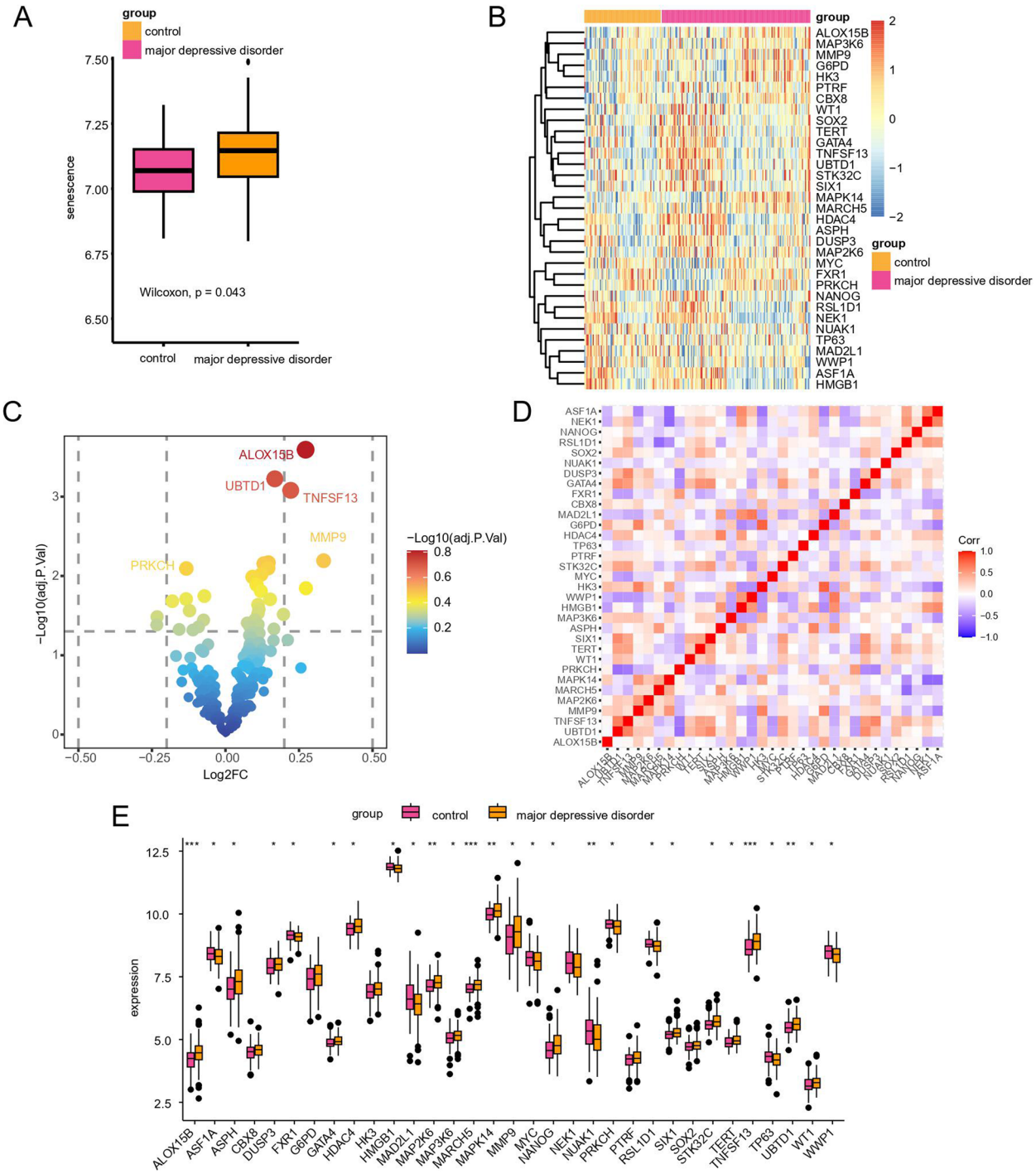


**Fig. 1** Analysis of Senescence-Related Differentially Expressed Genes (SR-DEGs) between MDD and Control Groups (**A**) GSVA analysis of senescence-related gene scores between MDD and control. **B** Heatmap of SR-DEGs between MDD and control. **C** Volcano plot of SR-DEGs between MDD and control. **D** Heatmap of correlation analysis of SR-DEGs. **E** Boxplot of SR-DEGs between MDD and control

differences between MDD and control groups (Fig. 1B-C, E). For example, *ALOX15B* and *UBTD1* were upregulated in MDD, while *PRKCH* was downregulated, indicating distinct roles in disease development. Furthermore, the correlation coefficients between the 33 SR-DEGs were also calculated (Fig. 1D). A strong positive correlation between *UBTD1* and *TNFSF13*, and a negative correlation between *UBTD1* and *PRKCH*, was observed.

### Establishment of the MDD diagnostic model based on the hub SRGs

We identified five hub SR-DEGs (*ALOX15B*, *TNFSF13*, *MARCH15*, *UBTD1*, and *MAPK14*) using RF and SVM-RFE methods (Fig. 2A-B). A logistic regression model created a diagnostic prediction model incorporating these hub genes. The model demonstrated an AUC of 0.763, indicating good potential for distinguishing MDD from controls (Fig. 2C-D). Bootstrap validation ($n=1000$) confirmed the reliability of the ROC (Fig. 2E). Also, we comparison of standardized net benefit demonstrating high risk threshold of different hub SR-DEGs (Fig. 2F).

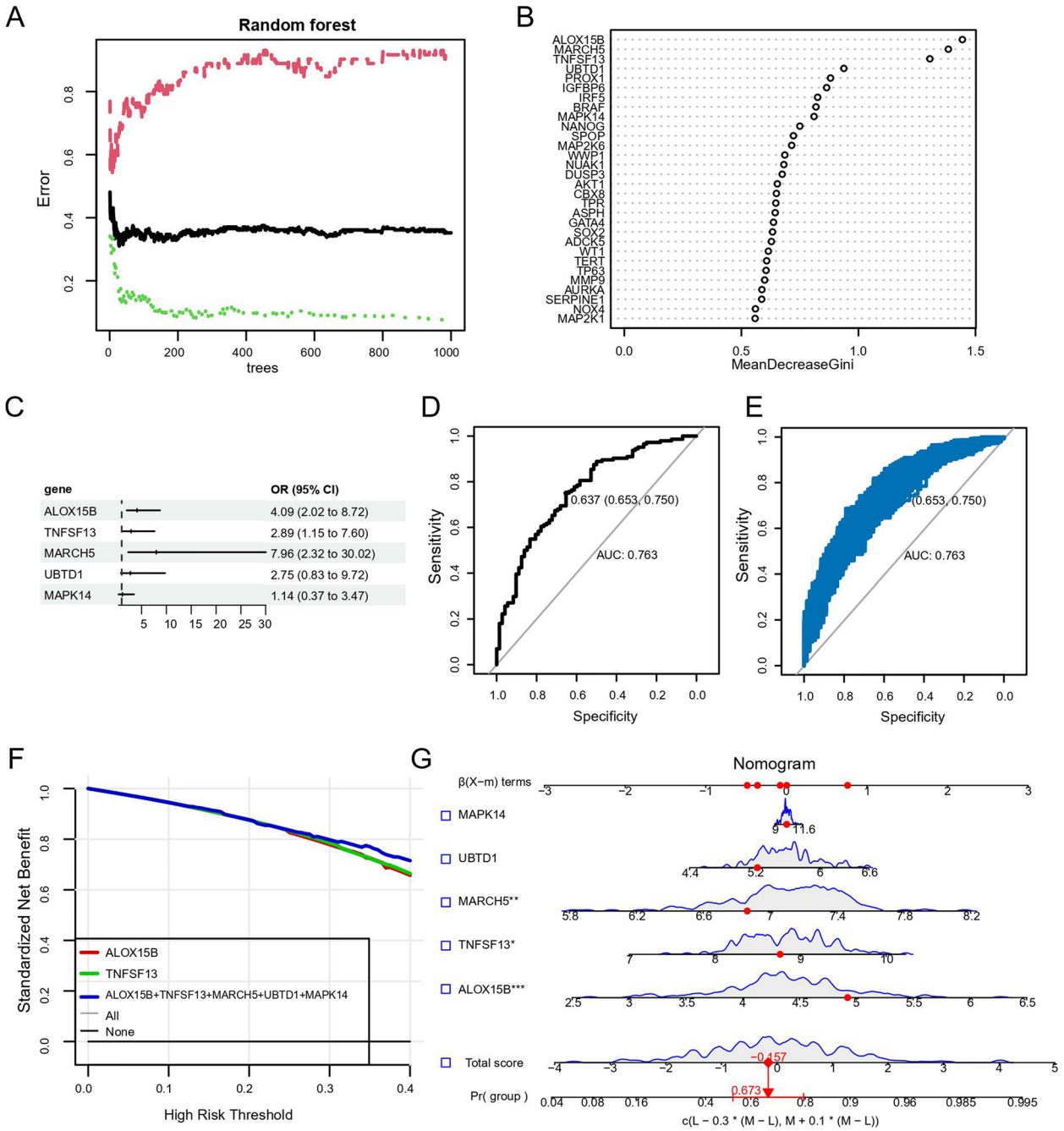


**Fig. 2** Establishment and capacity assessment of diagnostic model by hub SR-DEGs (**A**-**B**) The RF and SVM-RFE methods were applied to further screen hub SR-DEGs. **C** Forest plots for SR-DEGs in diagnostic model. **D** Receiver operating characteristic (ROC) curve of predicted risk scores in MDD diagnosis. **E** The AUC score for the full dataset was calculated and then 1000 bootstrap samples of the AUC score. **F** Comparison of standardized net benefit demonstrating high risk threshold of different hub SR-DEGs. **G** Nomogram of five hub SR-DEGs in the diagnosis of an MDD sample

The nomogram model based on these hub genes improved diagnostic precision, underscoring their significant contribution to MDD onset (Fig. 2G).

### Immune infiltration analysis

Immune cell infiltration analysis using IOBR revealed that MMP9 was positively correlated with neutrophils, M0 macrophages, and monocytes but inversely associated with memory B cells and resting memory CD4 T cells (Fig. 3A). The five hub genes demonstrated correlations with neutrophils, M2 macrophages, monocytes, regulatory T cells, and CD4 memory T cells (Fig. 3B). *MAPK14* was positively correlated with Neutrophils and M0 macrophages ($P<0.001$) and significantly negatively correlated with CD8 T cells ($P<0.001$). *ALOX15B* was positively correlated with Monocytes and negatively correlated with Neutrophils, Dendritic cells, and CD4 memory T cells ($P<0.001$). *TNFSF13* was significantly positively correlated with M2 macrophages, Monocytes, regulatory T cells and CD4 T cells ($P<0.001$), and significantly negatively correlated with CD4 memory T cells and B cells ($P<0.001$). *MARCH5* expression was positively correlated with Neutrophils and CD4 memory T cells ($P<0.001$), and negatively correlated with M2 macrophages, regulatory T cells, and CD8 T cells ($P<0.001$). *UBTD1* was positively correlated with Neutrophils, M2

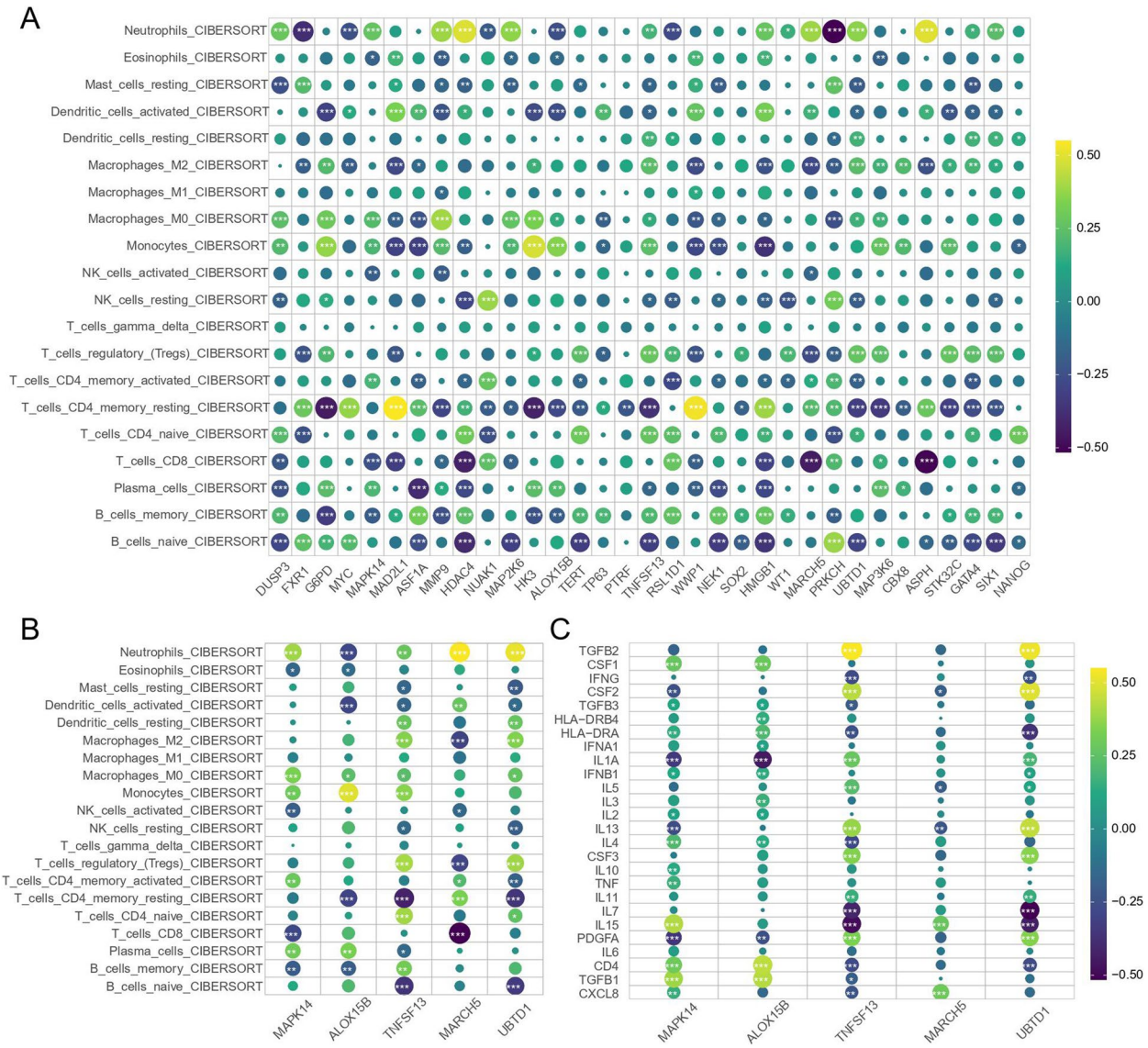


**Fig. 3** Immune infiltration analysis (**A**) The heatmap of the correlation of the 33 SRGs with the immune cells. **B** The heatmap of the correlation of the 5 hub SRGs with the immune cells. **C** The heatmap of the correlation of the 5 hub SRGs with the inflammatory factor

macrophages and regulatory T cells, and negatively correlated with CD4 memory T cells and B cells ($P < 0.001$). Correlation analysis between the hub genes and inflammatory factors indicated similar patterns for *UBTD1* and *TNFSF13*, suggesting analogous roles in immune regulation in MDD (Fig. 3C).

### Identification of two different MDD clusters

Consensus cluster analysis (Fig. 4A-B) identified two subgroups of MDD patients based on SRG expression patterns. GSEA enrichment analysis revealed that Cluster 2 induced pathways related to "regulation of complement activation" and "positive regulation of lymphocyte-mediated immunity", while these pathways were repressed in cluster 1 (Fig. 4C). Cluster 2 exhibited higher expression of *G6PD*, *MYC*, *MAPK14*, *MMP9*, *HK3*, *ALOX15B*, and *PRKCH*, and lower expression of *DUSP3*, *ASF1A*, and *TERT* (Fig. 4D). Additionally, cluster 2 showed increased expression of *CD4* and *TGFB1*, indicating heightened inflammatory marker levels (Fig. 4E).

### Identification of core modules between two MDD clusters

WGCNA was used to identify gene modules associated with the two MDD clusters. A quality control assessment of 144 MDD samples, retained all samples. Dynamic tree-cut analysis with a soft threshold identified significant co-expression modules (Fig. 5A-B). The turquoise module was positively correlated with cluster 2 and negatively correlated with cluster 1 ($p < 0.05$) (Fig. 5C). Metascape enrichment analysis of the turquoise module genes highlighted pathways such as "neutrophil degranulation", "positive regulation of immune response", and "translation" (Fig. 5D). Proteomap analysis revealed differential enrichment in pathways such

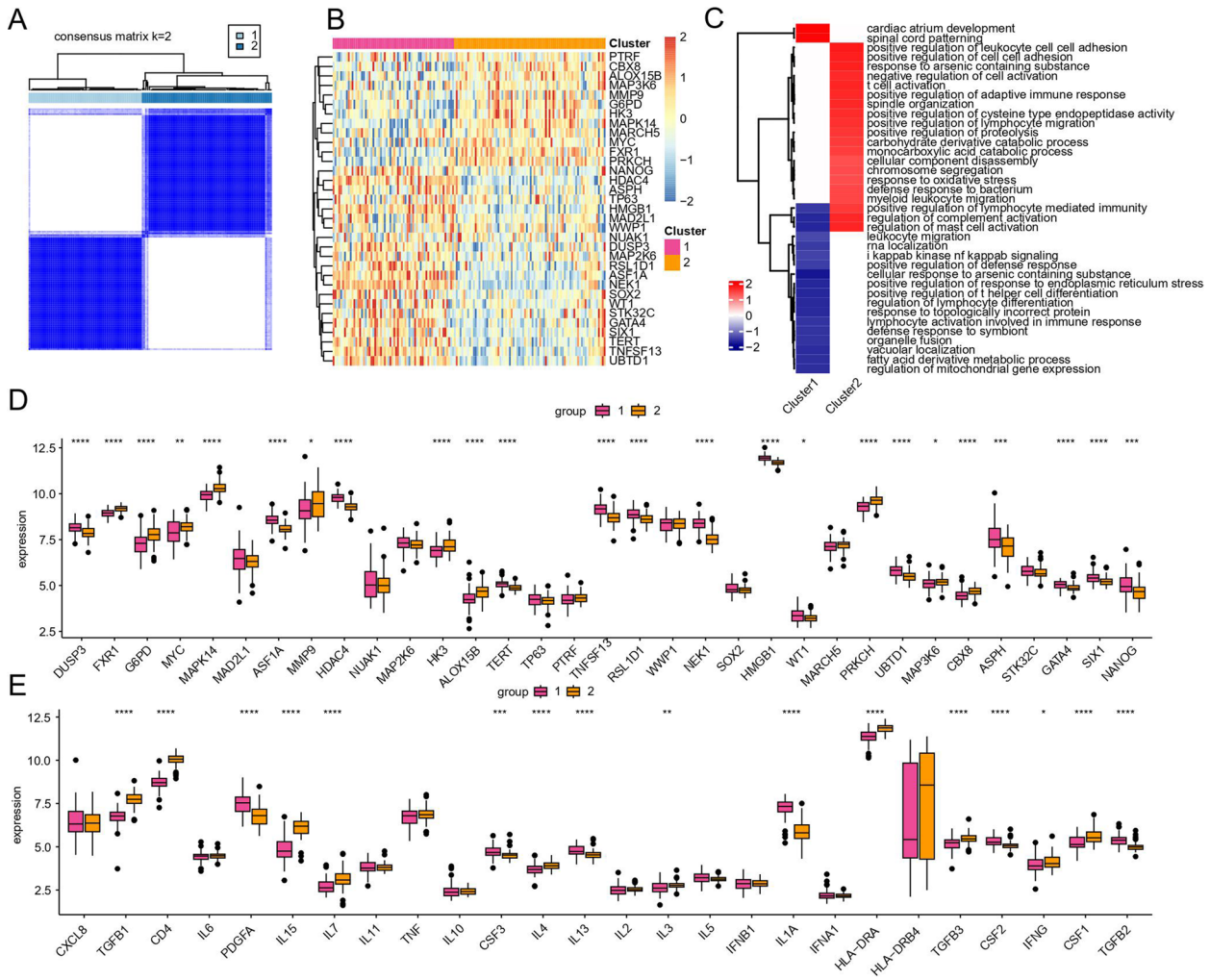


**Fig. 4** Consensus clustering analysis of MDD patients based on SRGs **A** Consensus matrix plots of consensus clustering for 144 MDD samples when k = 2. **B** Heat map of the SR-DEGs between the two clusters. **C** GSEA pathway differential analysis shows activated and inhibited pathways in the two clusters. **D** Box plot of SR-DEGs in the two clusters. **E** Differential expression of the inflammatory factors in the two clusters

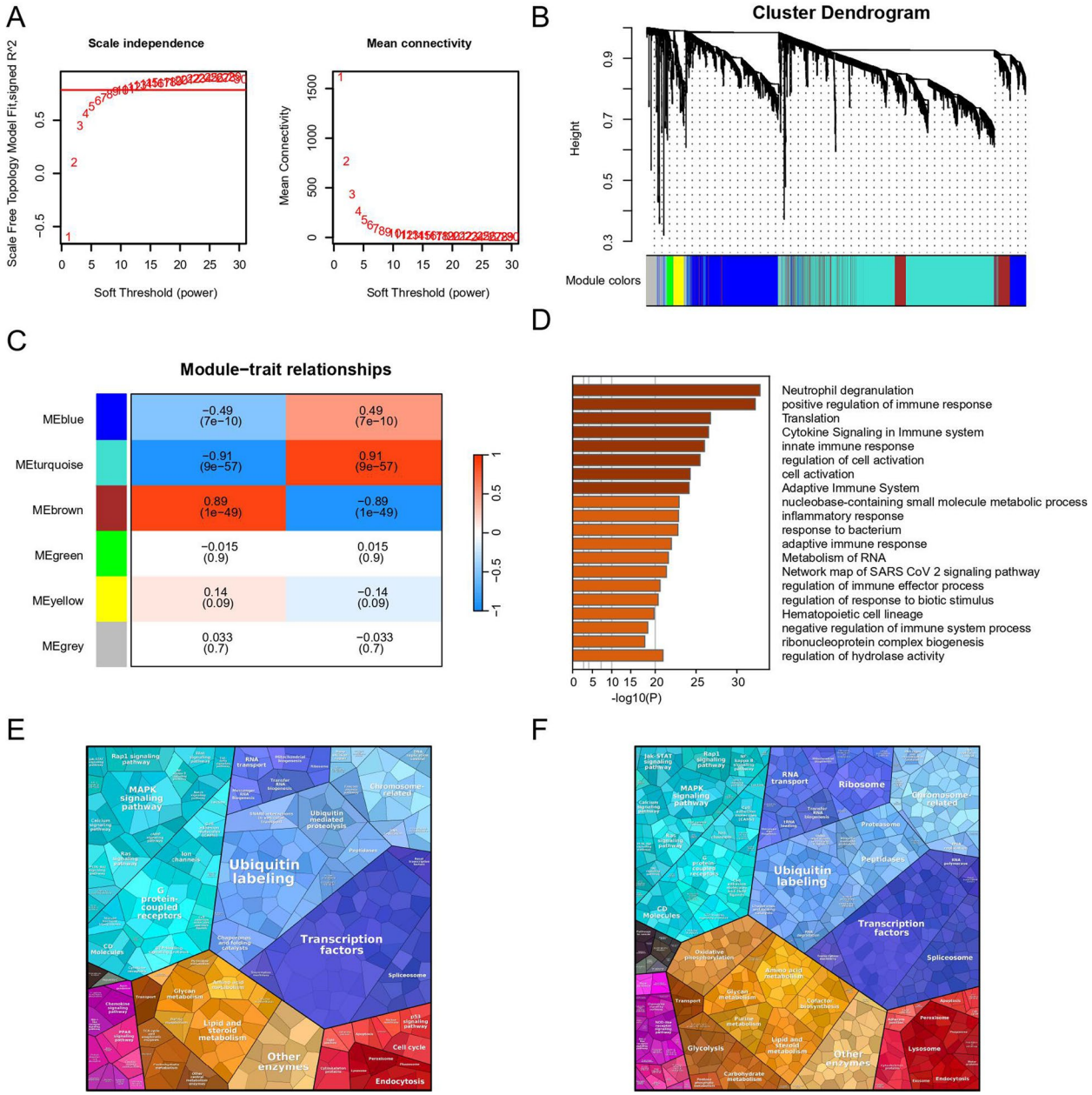


**Fig. 5** Weighted gene co-expression network analysis (WGCNA) (**A**) An analysis of the scale-free fit index and the mean connectivity for selected soft threshold powers (β). **B** Clustering dendrogram of genes based on topological overlapping. **C** Gene clustering dendrogram of WGCNA; (**D**) Enrichment analysis using Metascape for genes in the turquoise module. **E**-**F** Proteomics analysis of the proteins that were differently abundant between two clusters: E is cluster1 and F is cluster2

as oxidative phosphorylation, proteasome, RNA polymerase, and neuron active ligand-receptor interaction (Fig. 5E-F), elucidating potential mechanisms by which SRGs influence MDD progression.

### Single-cell analysis of SRGs in MDD

Utilizing the GSE144136 scRNA-seq dataset, we employed principal component analysis (PCA) to delineate 19 distinct cell clusters (Fig. 6A). These clusters predominantly encompassed mixed neurons (Mix), astrocytes (Astros), endothelial cells (Endo), excitatory cells (Ex), inhibitory cells (Inhib), macrophages/microglia (Micro/Macro), oligodendrocytes (Oligos), and oligodendrocyte precursor cells (OPCs) (Fig. 6B). The findings of the SRG score analysis indicated that endothelial cells exhibited the highest SRG score (Fig. 6C). In addition,

astrocytes exhibited a more substantial response to signals from high-senescence endothelial cells compared to those from low-senescence cells (Fig. 6D), and there was a notable activation of the Notch signaling pathway (Fig. 6E). The activation of Notch signaling, particularly through the DLL4-NOTCH1 and ADAM17-NOTCH1 pathways, was markedly observed transitioning from high-senescence endothelial cells to astrocytes (Fig. 6F-G), indicating the pivotal role of the Notch pathway in the progression of MDD.

### SCENIC analysis of high and low senescence endothelial cells

The SCENIC analysis compared transcription factors in endothelial cells with varying SRG scores. Transcription factors *ZEB1*, *NFAT5*, *FOXP1*, and *NFIA* were associated with low senescence scores, whereas *LEF1*, *KLF2*, *FOXP1*, and *FLI1* were linked to high senescence scores (Fig. 7A-B). Correlation analysis demonstrated that SRGs positively correlated with transcription factors associated with high senescence scores (Fig. 7C), underscoring the importance of transcription factors in regulating senescence in MDD.

## Discussion

MDD is a multifaceted and incapacitating condition, widely recognized as the primary cause of disability on a global scale [36, 37]. Despite its prevalence, the precise mechanisms underlying MDD remain incompletely elucidated. Recent investigations leveraging advanced sequencing technologies have endeavored to elucidate the etiology of MDD and pinpoint potential diagnostic biomarkers [38, 39], highlighting the potential link between senescence and immunity in the development

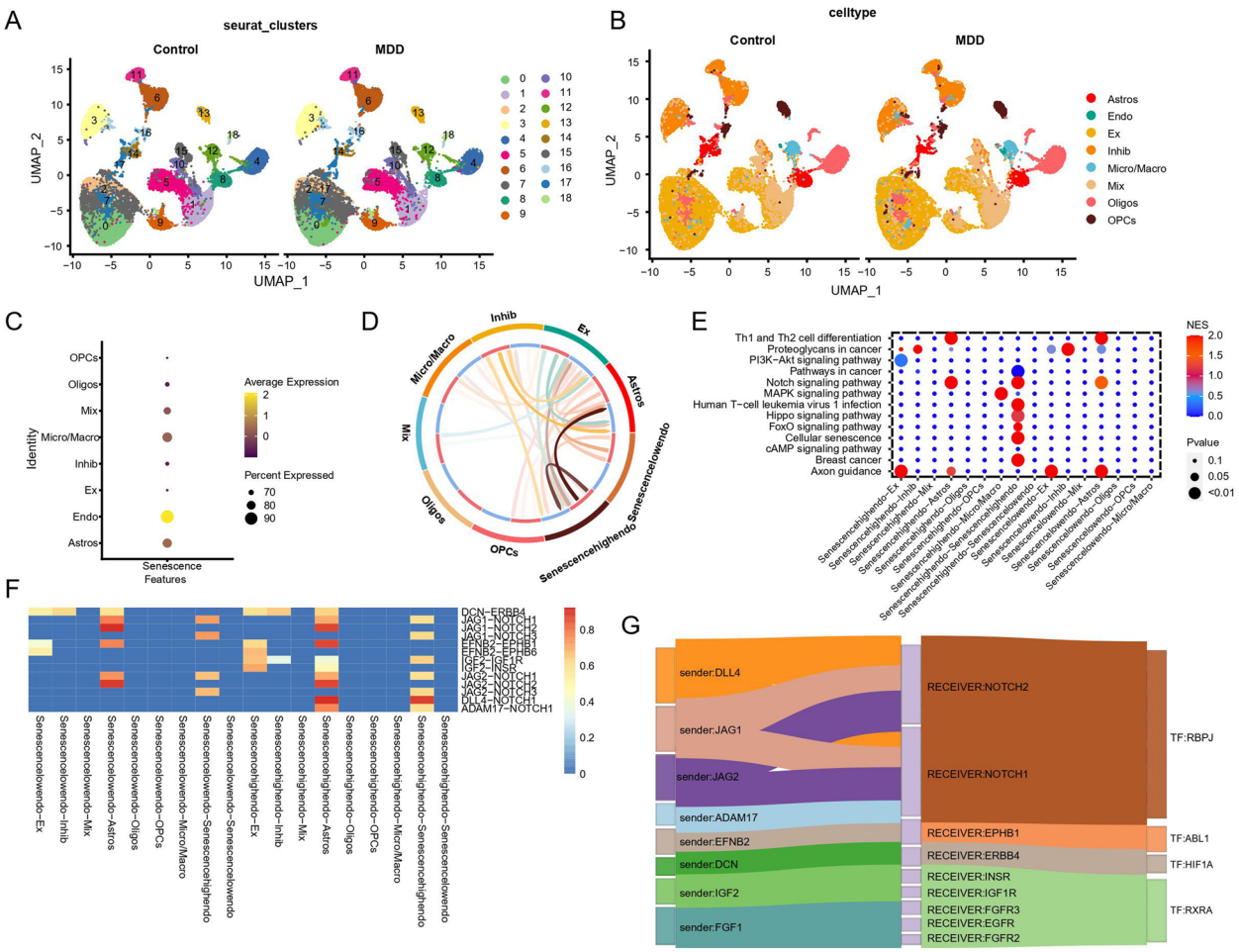


**Fig. 6** Single-cell analysis of SRGs in MDD and detailed analysis of cell-cell communications (**A**-**B**) UMAP plot of different cell types in the MDD and control. **C** The dot plot of UCell scores of SRGs in the different cell types. **D** Cell communication analysis among high and low senescence endothelial cells with other cells. **E** CellCall analysis determined pathway differences between high and low senescence endothelial cells with other cells. **F** The intercellular communications from high senescence endothelial cells to astrocytes. **G** The Sankey plot of the intercellular communications from high senescence endothelial cells to astrocytes

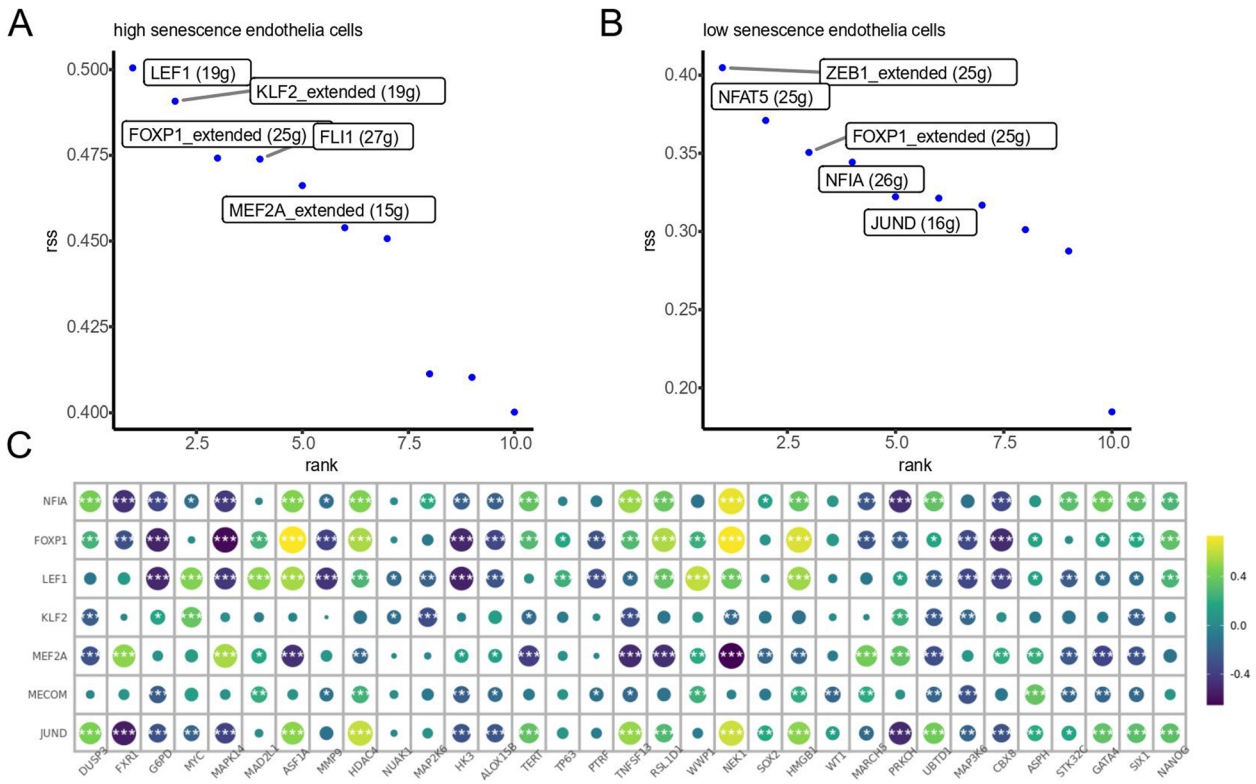


**Fig. 7** Transcription factor profiles correlation analysis with SRGs in high and low senescence endothelial cells (**A**-**B**) Transcription factor profiles in high and low senescence endothelial cells. **C** Correlation analysis between the 7 transcription factors unique to 33 SR-DEGs

of depression [40, 41]. In this research, we employed diverse bioinformatic methodologies to delineate biomarkers linked to senescence in MDD and conducted a comprehensive analysis of the role of SRGs at a cellular level. Our findings indicate that distinct SRGs exhibit varying expression patterns in individuals with MDD, potentially indicating an interrelation between alterations in cellular function during senescence and the pathophysiology of MDD. These genes may play a role in modulating the inflammatory response, oxidative stress, and neuroplasticity changes characteristic of MDD. These common pathological pathways may serve as the mechanistic foundation for the involvement of senescent cells in the progression of MDD.

Our investigation unveiled a pronounced upregulation in the expression of gene sets associated with senescence in MDD samples, as evidenced by GSVA analysis. The results of GSVA analysis indicate that the expression levels of genes related to senescence are heightened in individuals with MDD, hinting at an accelerated senescence process in this population.This finding aligns with prior research indicating premature aging features in MDD patients, such as telomere shortening and elevated inflammatory markers. Leveraging five hub SR-DEGs, we constructed a predictive model for MDD, achieving a notable AUC score of 0.763, denoting high diagnostic efficacy.This model enabled the stratification of MDD patients into two distinct subgroups with marked discrepancies in gene expression profiles and immune cell infiltration. These subgroups exhibited noticeable differences in the expression patterns of specific genes identified as significantly regulated genes. Further single-cell analysis provided deeper insights into the intricate connections between senescence, cellular communication, and immunity in MDD.

The prediction model incorporated five shub SR-DEGs, *ALOX15B*, *TNFSF13*, *UBTD1*, *MARCH5*, and *MAPK14*. These genes were identified using machine learning methods idebtifiers to SVM and RF algorithms. Notably, these genes showed strong correlations with certain immune cells, suggesting their role in immunological regulation in MDD. For instance, *ALOX15B* plays a role in fatty acid metabolism and inflammation, is a crucial factor in ferroptosis, a process linked to MDD progression [42]. Suppressing ferroptosis has been demonstrated to ameliorate MDD, highlighting *ALOX15B*'s potential therapeutic importance. *TNFSF13*, a cytokine involved in immune response regulation, and UBTD1, associated with oxidative stress and protein breakdown, were

also highly expressed in MDD samples, emphasizing their relevance to the disease [43, 44]. Ubiquitin domain containing 1 (*UBTD1*) is a ubiquitin-like protein, which encodes a protein that is thought to regulate E2 ubiquitin-conjugases belonging to the *UBE2D* family. Studies have shown that *UBTD1* can induce cell senescence and regulate the expression of p53 protein [45]. It has also been shown that *UBTD1* plays an important regulatory role in the phosphorylation of EGFR and its lysosomal degradation [46]. At present, further experimental studies are needed to verify the mechanism of *UBTD1* and depression. membrane-associated ring-CH (*MARCH*) family belongs to a family of RING finger domains of E3 ubiquitin ligases. *MARCH5* is a mitochondrial ubiquitin ligase, also known as MITOL, which can be expressed in brain, heart, liver and other tissues [47]. *MARCH5* plays a role in maintaining mitochondrial homeostasis and preventing cellular senescence by regulating and acetylating Mfn1 [48–50]. MITOL by Yonashiro et al. can block S-nitroso MAP1B-light chain 1 (LC1) -mediated mitochondrial dysfunction and neuronal cell death [51]. It is speculated that MARCH5 may be involved in the pathogenesis of depression by regulating Mfn2. Mitogen-activated protein kinases (*MAPK*) family members are serine/threonine protein kinases, It is involved in cell cycle regulation, apoptosis, cell development, proliferation and inflammatory response [52]. *MAPK14* is considered to be the central regulator of inflammatory response in various cell types [53]. Zhang J et al. also found that *MAPK14* was a potential biomarker of depression in their comprehensive analysis of endoplasmic reticulum emergency and immune infiltration in major depression [54]. We speculate that *MAPK14* may be involved in the progression of depression by regulating endoplasmic reticulum and inflammatory response.

Our research further establishes a connection central SRGs expression to the immunological environment and inflammatory factors. Hub SR-DEGs exhibited positive correlations with neutrophils and negatively with CD4 memory resting T cells and CD8 + T cells, while showing the interplay between senescence and immune response in MDD. A notable correlation between TGFB2 and hub SRGs, implying TGFB2's role in MDD senescence through the TGF-B2-SMAD2/3-p53-p21 WAF1/CIP1-mediated RB pathway [55]. Additionally, our study identified two MDD subtypes based on SRGs expression patterns, which could provide insights for patient categorization and personalized treatment approaches.

Single-cell analysis of SRGs in MDD provided further understanding of this complex disorder. Endothelial cells are an important part of blood vessels, and senescent endothelial cells are very active, showing a high degree of secretion and pro-inflammatory. Barinda AJ et al. found that endothelial cell senescence leads to elevated expression of inflammatory cytokines and ROS and induces senescence of surrounding healthy cells in a positive feedback manner, thereby propagating and perpetuating the inflammatory microenvironment [56]. However, it has also been shown that senescent endothelial cells produce many inflammatory chemokines and cytokines, including IL-1β, IL-6, IL-8, CXCL11 and plasminogen activator inhibitor 1 (PAI1), reduced the expression of anti-inflammatory IL-10, and increased the expression of multiple cell adhesion molecules [57–62]. These lines of evidence suggest a complex interplay between inflammation and endothelial cell senescence [63]. In addition, Venkatesh D et al. found that endothelial cells in human and mouse atherosclerotic plaques upregulated notch receptor 1 (Notch1) signaling, which promoted the expression of ICAM1, IL-1α, IL-6 and IL-8 and the transepithelial migration of monocytes [64]. Our study also found that endothelial cells exhibited the highest senescence score and that highly senescent endothelial cells initiated novel cell-astrocyte interactions, again via Notch signaling. Mathias Linnerbauer's research had shown that the cross-linking of astrocytes and endothelial cells is essential for limiting leukocyte migration to parenchymal cells [65]. In the context of neuroinflammation, bidirectional communication between astrocytes and endothelial cells would promote BBB leakage and allow infiltration of peripheral immune cells [66]. Argaw and colleagues demonstrated that VEGF-A production in astrocytes is upregulated in response to IL-1b, a cytokine produced by activated microglia during neuroinflammation [67]. VEGF-A induces the endothelial nitric oxide synthase (eNOS)-dependent downregulation of tight-junction proteins claudin-5 (Cldn5) and occludin (Ocln) in endothelial cells, which eventually disrupts tight-junctions and BBB integrity [68, 69]. Astrocytes also produce factors that boost BBB integrity during inflammatory conditions. For example, astrocytes promote BBB stability via the production of sonic-hedgehog (Shh) [70]. These interactions, including the DLL4-NOTCH1 and ADAM17-NOTCH1 receptor pairs, suggest that senescent endothelial cells communicate with astrocytes through pathways critical for immune regulation.

We also discovered distinct transcription factor profiles between high and low-senescence endothelial cells. Key transcription factors such as LEF1(+) showed a positive relationship with SRG genes in high senescence cells, indicating their role in controlling mitochondrial autophagy and suggesting a significant function in MDD pathogenesis. Conversely, FOXP1 plays a complex role in senescence, which may depend on cell type, tissue environment, or specific biological conditions. The function of FOXP1 may be influenced

by its binding partner, epigenetic modifications, and the genomic region to which it binds. FOXP1 may affect the senescence state of cells through different mechanisms in different cellular or tissue backgrounds, which is worthy of further exploration [71, 72].

Nonetheless, there are several limitations of our study that need to be considered. First, the study's reliance on publicly available data sets may introduce biases related to sample selection and data quality. Because the data come from different studies and platforms, there are batch effects and platform differences, which may affect the measurement of gene expression and the accuracy of the analysis results. Second, while random forest and SVM recursive feature elimination are powerful feature selection methods, their results may be affected by parameter Settings and model assumptions. Different algorithms may lead to different feature selection results. In addition, there are confounding factors such as demographic and clinical variables, medication use and comorbidities, which may not be fully controlled in the analysis. Finally, experimental validation of the genes we have identified could further enhance our findings.

In conclusion, our study has identified five novel SR-DEGs play a crucial role in MDD progression. These genes offer potential as therapeutic targets and diagnostic markers, thus propelling the advancement the field of precision medicine for MDD.

## Supplementary Information

The online version contains supplementary material available at https://doi.org/10.1186/s12888-025-06542-8.

Supplementary Material 1.

Supplementary Material 2.

**Acknowledgements**
The authors would like to thank all subjects who participated in this study. In particular, we thank Bioinfo_composer, the leading bioinformatics team in China, for their selfless help.

**Authors' contributions**
Kun Lian: Writing – original draft. Wei Yang: Conceptualization, Editing. Jing Ye: Writing –methodology, Data curation. Yilan Chen: Methodology. Lei Zhang: Statistical analysis. Xiufeng Xu: Supervision, Resources, Writing – review & editing.All authors reviewed the manuscript.

**Funding**
This study was funded by the Yunnan Clinical Research Center for Mental Disorders (202102AA100058) the Medical Joint Special Project of Kunming University of Science and Technology and the Second People's Hospital of Yuxi(KUST-YX2022002).

**Data availability**
The raw data supporting the findings of this article is available in the GEO dataset (GSE32280 and GSE98793) and the scRNA-seq data from GSE144136.

## Declarations

**Ethics approval and consent to participate**
The patients involved in the GEO database have obtained ethical approval. Our study is based on open data, there are no ethical issues and other conflicts of interest.

**Competing interests**
The authors declare no competing interests.

Received: 3 July 2024 Accepted: 28 January 2025
Published online: 03 March 2025

**References**

1. Lim GY, Tam WW, Lu Y, et al. Prevalence of depression in the community from 30 countries between 1994 and 2014. Sci Rep. 2018;8(1):2861.
2. Davis AK, Barrett FS, May DG, et al. Effects of psilocybin-assisted therapy on major depressive disorder: a randomized clinical trial. JAMA Psychiatry. 2021;78(5):481–9.
3. Uchida S, Yamagata H, Seki T, et al. Epigenetic mechanisms of major depression: targeting neuronal plasticity. Psychiatry Clin Neurosci. 2018;72(4):212–27.
4. Yuan M, Yang B, Rothschild G, et al. Epigenetic regulation in major depression and other stress-related disorders: molecular mechanisms, clinical relevance and therapeutic potential. Signal Transduct Target Ther. 2023;8(1):309.
5. Hasin DS, Sarvet AL, Meyers JL, et al. Epidemiology of adult DSM-5 major depressive disorder and its specifiers in the United States. JAMA Psychiatry. 2018;75(4):336–46.
6. Anwar T, Khosla S, Ramakrishna G. Increased expression of SIRT2 is a novel marker of cellular senescence and is dependent on wild type p53 status. Cell Cycle. 2016;15(14):1883–97.
7. Lucas V, Cavadas C, Aveleira CA. Cellular senescence: from mechanisms to current biomarkers and senotherapies. Pharmacol Rev. 2023;75(4):675–713.
8. Ridout KK, Ridout SJ, Price LH, et al. Depression and telomere length: a meta-analysis. J Affect Disord. 2016;191(2):237–47.
9. Wu Y, Huang C, Fan B, et al. The relationship between leukocyte telomere length and risk of depression and anxiety: evidence from UK Biobank. J Affect Disord. 2025;369(1):195–201.
10. Pisanu C, Congiu D, Meloni A, et al. Dissecting the genetic overlap between severe mental disorders and markers of cellular aging: identification of pleiotropic genes and druggable targets. Neuropsychopharmacology. 2024;49(6):1033–41.
11. Richmond-Rakerd LS, D'Souza S, Milne BJ, et al. Longitudinal associations of mental disorders with physical diseases and mortality among 2.3 million New Zealand citizens. JAMA Netw Open. 2021;4(1):e2033448.
12. Sinclair LI, Mohr A, Morisaki M, et al. Is later-life depression a risk factor for Alzheimer's disease or a prodromal symptom: a study using post-mortem human brain tissue? Alzheimers Res Ther. 2023;12(151):153.
13. Richmond-Rakerd LS, D'Souza S, Milne BJ, et al. Longitudinal associations of mental disorders with dementia: 30-year analysis of 1.7 million New Zealand citizens. JAMA Psychiatry. 2022;79(4):333–40.
14. Soysal P, Veronese N, Thompson T, et al. Relationship between depression and frailty in older adults: a systematic review and meta-analysis. Ageing Res Rev. 2017;36(6):78–87.
15. Leday GGR, Vértes PE, Richardson S, et al. Replicable and coupled changes in innate and adaptive immune gene expression in two case-control studies of blood microarrays in major depressive disorder. Biol Psychiatry. 2018;83(1):70–80.
16. Hu G, Yu S, Yuan C, et al. Gene expression signatures differentiating major depressive disorder from subsyndromal symptomatic depression. Aging. 2021;13(9):13124–37.
17. Leek JT, Johnson WE, Parker HS, et al. The sva package for removing batch effects and other unwanted variation in high-throughput experiments. Bioinformatics. 2012;28(6):882–3.

18. Tacutu R, Thornton D, Johnson E, et al. Human ageing genomic resources: new and updated databases. Nucleic Acids Res. 2018;46(D1):D1083-90.
19. Ritchie ME, Phipson B, Wu D, et al. Limma powers differential expression analyses for RNA-sequencing and microarray studies. Nucleic Acids Res. 2015;43(7):e47.
20. Hänzelmann S, Castelo R, Guinney J. GSVA: gene set variation analysis for microarray and RNA-seq data. BMC Bioinformatics. 2013;14(1): 7.
21. Ferreira JA. Models under which random forests perform badly; consequences for applications. Comput Stat. 2022;37(1):1839–54.
22. Sanz H, Valim C, Vegas E, et al. SVM-RFE: selection and visualization of the most relevant features through non-linear kernels. BMC Bioinformatics. 2018;19(1):432.
23. Robin X, Turck N, Hainard A, et al. pROC: an open-source package for R and S+to analyze and compare ROC curves. BMC Bioinformatics. 2011;12(3):77.
24. Zeng D, Ye Z, Shen R, et al. IOBR: multi-omics immuno-oncology biological research to decode tumor microenvironment and signatures. Front Immunol. 2021;12(7):687975.
25. Becht E, Giraldo NA, Lacroix L, et al. Estimating the population abundance of tissue-infiltrating immune and stromal cell populations using gene expression. Genome Biol. 2016;17(1):218.
26. Yang W, Lian K, Ye J, et al. Analyses of single-cell and bulk RNA sequencing combined with machine learning reveal the expression patterns of disrupted mitophagy in schizophrenia. Front Psychiatry. 2024;17(9):1429437.
27. Langfelder P, Horvath S. WGCNA: an R package for weighted correlation network analysis. BMC Bioinformatics. 2008;9(12):559.
28. Castanza AS, Recla JM, Eby D, et al. Extending support for mouse data in the molecular signatures database (MSigDB). Nat Methods. 2023;20(11):1619–20.
29. Zhou Y, Zhou B, Pache L, et al. Metascape provides a biologist-oriented resource for the analysis of systems-level datasets. Nat Commun. 2019;10(1):1523.
30. Reis-de-Oliveira G, Carregari VC, Sousa GRDR, et al. OmicScope unravels systems-level insights from quantitative proteomics data. Nat Commun. 2024;15(1):6510.
31. Nagy C, Maitra M, Tanti A, et al. Single-nucleus transcriptomics of the prefrontal cortex in major depressive disorder implicates oligodendrocyte precursor cells and excitatory neurons. Nat Neurosci. 2020;23(6):771–81.
32. Andreatta M, Carmona SJ, UCell. Robust and scalable single-cell gene signature scoring. Comput Struct Biotechnol J. 2021;19(1):3796–8.
33. Bravo GBC, De Winter S, Hulselmans G, et al. SCENIC+: single-cell multiomic inference of enhancers and gene regulatory networks. Nat Methods. 2023;20(9):1355–67.
34. Wu X, Yang X, Dai Y, et al. Single-cell sequencing to multi-omics: technologies and applications. Biomark Res. 2024;12(1):110.
35. Zhang Y, Liu T, Hu X, et al. CellCall: integrating paired ligand-receptor and transcription factor activities for cell-cell communication. Nucleic Acids Res. 2021;49(15):8520–34.
36. Anderson E, Crawford CM, Fava M, et al. Depression - understanding, identifying, and diagnosing. N Engl J Med. 2024;390(17):e41.
37. Athira KV, Bandopadhyay S, Samudrala PK, et al. An overview of the heterogeneity of major depressive disorder: current knowledge and future prospective. Curr Neuropharmacol. 2020;18(3):168–87.
38. Ning L, Yang Z, Chen J, et al. A novel 4 immune-related genes as diagnostic markers and correlated with immune infiltrates in major depressive disorder. BMC Immunol. 2022;23(1):6.
39. Zhang G, Xu S, Zhang Z, et al. Identification of key genes and the pathophysiology associated with major depressive disorder patients based on integrated bioinformatics analysis. Front Psychiatry. 2020;11(3): 192.
40. Debnath M, Berk M, Maes M. Translational evidence for the inflammatory response system (IRS)/Compensatory Immune Response System (CIRS) and neuroprogression theory of major depression. Prog Neuropsychopharmacol Biol Psychiatry. 2021;111(12):110343.
41. Schroder JD, de Araújo JB, de Oliveira T, et al. Telomeres: the role of shortening and senescence in major depressive disorder and its therapeutic implications. Rev Neurosci. 2021;33(3):227–55.
42. Zhou Y, Huang Y, Ye W, et al. Cynaroside improved depressive-like behavior in CUMS mice by suppressing microglial inflammation and ferroptosis. Biomed Pharmacother. 2024;173(4):116425.
43. Cruz-Pereira JS, Rea K, Nolan YM, et al. Depression's unholy trinity: dysregulated stress, immunity, and the microbiome. Annu Rev Psychol. 2020;71(1):49–78.
44. Bhatt S, Nagappa AN, Patil CR. Role of oxidative stress in depression. Drug Discov Today. 2020;25(7):1270–6.
45. Zhang XW, Wang XF, Ni SJ, et al. UBTD1 induces cellular senescence through an UBTD1-Mdm2/p53 positive feedback loop. J Pathol. 2015;235(4):656–67.
46. Torrino S, Tiroille V, Dolfi B, et al. UBTD1 regulates ceramide balance and endolysosomal positioning to coordinate EGFR signaling. Elife. 2021;10(4):e68348.
47. Nakamura N, Kimura Y, Tokuda M, et al. MARCH-V is a novel mitofusin 2- and Drp1-binding protein able to change mitochondrial morphology. EMBO Rep. 2006;10:1019–22.
48. Shiiba I, Takeda K, Nagashima S, et al. MITOL promotes cell survival by degrading Parkin during mitophagy. EMBO Rep. 2021;22(3): e49097.
49. Nagashima S, Tokuyama T, Yonashiro R, et al. Roles of mitochondrial ubiquitin ligase MITOL/MARCH5 in mitochondrial dynamics and diseases. J Biochem. 2014;155(5):273–9.
50. Koyano F, Yamano K, Kosako H, et al. Parkin-mediated ubiquitylation redistributes MITOL/March5 from mitochondria to peroxisomes. EMBO Rep. 2019;20(12):e47728.
51. Yonashiro R, Kimijima Y, Shimura T, et al. Mitochondrial ubiquitin ligase MITOL blocks S-nitrosylated MAP1B-light chain 1-mediated mitochondrial dysfunction and neuronal cell death. Proc Natl Acad Sci U S A. 2012;109(7):2382–7.
52. Lo U, Selvaraj V, Plane JM, et al. p38α (MAPK14) critically regulates the immunological response and the production of specific cytokines and chemokines in astrocytes. Sci Rep. 2014;4(12):7405.
53. Kim C, Sano Y, Todorova K, et al. The kinase p38 alpha serves cell type-specific inflammatory functions in skin injury and coordinates pro- and anti-inflammatory gene expression. Nat Immunol. 2008;9(9):1019–27.
54. Madkour MM, Anbar HS, El-Gamal MI. Current status and future prospects of p38α/MAPK14 kinase and its inhibitors. Eur J Med Chem. 2021;213(5):113216.
55. Zheng H, Liu M, Shi S, et al. MAP4K4 and WT1 mediate SOX6-induced cellular senescence by synergistically activating the ATF2-TGFβ2-Smad2/3 signaling pathway in cervical cancer. Mol Oncol. 2024;18(5):1327–46.
56. Barinda AJ, Ikeda K, Nugroho DB, et al. Endothelial progeria induces adipose tissue senescence and impairs insulin sensitivity through senescence associated secretory phenotype. Nat Commun. 2020;11(1):481.
57. Khan SY, Awad EM, Oszwald A, et al. Premature senescence of endothelial cells upon chronic exposure to TNFα can be prevented by N-acetyl cysteine and plumericin. Sci Rep. 2017;7(1): 39501.
58. Zhao N, Li CC, Di B, et al. Recent advances in the NEK7-licensed NLRP3 inflammasome activation: mechanisms, role in diseases and related inhibitors. J Autoimmun. 2020;113(9):102515.
59. Bent EH, Gilbert LA, Hemann MT. A senescence secretory switch mediated by PI3K/AKT/mTOR activation controls chemoprotective endothelial secretory responses. Genes Dev. 2016;30(16):1811–21.
60. Ya J, Bayraktutan U. Vascular ageing: mechanisms, risk factors, and treatment strategies. Int J Mol Sci. 2023;24(14): 11538.
61. Hwang HJ, Lee YR, Kang D, et al. Endothelial cells under therapy-induced senescence secrete CXCL11, which increases aggressiveness of breast cancer cells. Cancer Lett. 2020;490(10):100–10.
62. Shaikh SB, Balaya RDA, Dagamajalu S, et al. A signaling pathway map of plasminogen activator inhibitor-1 (PAI-1/SERPINE-1): a review of an innovative frontier in molecular aging and cellular senescence. Cell Commun Signal. 2024;22(1):544.
63. Bloom SI, Islam MT, Lesniewski LA, et al. Mechanisms and consequences of endothelial cell senescence. Nat Rev Cardiol. 2023;20(1):38–51.
64. Venkatesh D, Fredette N, Rostama B, et al. RhoA-mediated signaling in notch-induced senescence-like growth arrest and endothelial barrier dysfunction. Arterioscler Thromb Vasc Biol. 2011;31(4):876–82.
65. Linnerbauer M, Wheeler MA, Quintana FJ. Astrocyte crosstalk in CNS inflammation. Neuron. 2020;108(4):608–22.
66. Abbott N, Rönnbäck L, Hansson E. Astrocyte–endothelial interactions at the blood–brain barrier. Nat Rev Neurosci. 2006;7(1):41–53.
67. Argaw AT, Asp L, Zhang J, et al. Astrocyte-derived VEGF-A drives blood-brain barrier disruption in CNS inflammatory disease. J Clin Invest. 2012;122(7):2454–68.

68. Wheeler MA, Clark IC, Tjon EC, et al. MAFG-driven astrocytes promote CNS inflammation. Nature. 2021;578(7796):593–9.
69. Alvarez JI, Dodelet-Devillers A, Kebir H, et al. The hedgehog pathway promotes blood-brain barrier integrity and CNS immune quiescence. Science. 2011;334(6063):1727–31.
70. Honda S, Ikeda K, Urata R, et al. Cellular senescence promotes endothelial activation through epigenetic alteration, and consequently accelerates atherosclerosis. Sci Rep. 2021;11(1):14608.
71. Chasse R, McLeod R, Surian A, et al. The role of cerebellar FOXP1 in the development of motor and communicative behaviors in mice. Genes Brain Behav. 2024;23(5): e70001.
72. Khandelwal N, Kulkarni A, Ahmed NI, et al. FOXP1 regulates the development of excitatory synaptic inputs onto striatal neurons and induces phenotypic reversal with reinstatement. Sci Adv. 2024;10(18): eadm7039.

## Publisher's Note